Article

Histopathological Insights and Therapeutic Prospects of MCC950 in Diabetic Cardiac Autonomic Neuropathy in a Type 1 Diabetes Wistar Rat Model

Shamala Devi Subramaniam , Juita Chupri , Zamzarina Ahmad Bajari , Kah Hui Wong , Mohd Amir Kamaruzzaman * , Razif Abas *

Posted Date: 25 September 2024

doi: 10.20944/preprints202409.1907.v1

Keywords: Diabetic Cardiac Autonomic Neuropathy (DCAN); Type 1 Diabetes Mellitus (T1DM); MCC950; NLRP3 Inflammasome; Histopathology

Article

Histopathological Insights and Therapeutic Prospects of MCC950 in Diabetic Cardiac Autonomic Neuropathy in a Type 1 Diabetes Wistar Rat Model

Shamala Devi Subramaniam [1], Juita Chupri [2], Zamzarina Ahmad Bajari [2], Wong Kah Hui [3], Muhammad Amir Kamaruzzaman [4,*] and Razif Abas [5,*]

[1] Department of Medical Microbiology, Faculty of Medicine and Health Sciences, Universiti Putra Malaysia, 43400 Serdang, Selangor, Malaysia
[2] Department of Pathology, Faculty of Medicine and Health Sciences, Universiti Putra Malaysia, 43400 Serdang, Selangor, Malaysia
[3] Department of Anatomy, Faculty of Medicine, University Malaya, 50603 Kuala Lumpur, Malaysia
[4] Department of Anatomy, Faculty of Medicine, Universiti Kebangsaan Malaysia, 56000 Cheras, Kuala Lumpur, Malaysia
[5] Department of Human Anatomy, Faculty of Medicine and Health Sciences, Universiti Putra Malaysia, 43400 Serdang, Selangor, Malaysia
* Correspondence: mohdamir@ukm.edu.my (M.A.K.); razifabas@upm.edu.my (R.A.); Tel.: +60391458605 (M.A.K.); +60397692479 (R.A.)

Abstract: Diabetic cardiac autonomic neuropathy (DCAN) is a severe complication of type 1 diabetes mellitus (T1DM) characterized by autonomic nerve fiber dysfunction in the heart and blood vessels. This study aimed to elucidate the histopathological mechanisms underlying DCAN and evaluate the therapeutic potential of MCC950, an NLRP3 inflammasome inhibitor, in a Wistar rat model. Male Wistar rats were divided into control and T1DM groups, with diabetes induced by streptozotocin (STZ) injection. Following confirmation of DCAN through elevated serum noradrenaline levels, diabetic rats were subdivided into positive control (insulin-treated), treatment (MCC950), and untreated groups. The stellate ganglia, thoracic aorta, and left ventricle were dissected for histological examination using Haematoxylin and Eosin (H&E) and Masson Trichrome staining. STZ-induced hyperglycemia was evident by Week 2 and sustained throughout the study. Serum noradrenaline levels significantly increased by Week 14 in diabetic rats, indicating DCAN onset. Histological analysis revealed atrophy in stellate ganglia, endothelial damage in the thoracic aorta, and myocardial fibrosis in untreated diabetic rats. MCC950 treatment preserved ganglionic structure, mitigated vascular damage, and reduced myocardial fibrosis, demonstrating its potential in attenuating DCAN progression. These findings highlight MCC950 as a promising therapeutic agent for DCAN by targeting inflammation and preserving autonomic and cardiovascular function. Further investigations are warranted to validate MCC950's efficacy in human trials, with the potential to improve clinical outcomes for T1DM patients at risk of DCAN.

Keywords: diabetic cardiac autonomic neuropathy (DCAN); type 1 diabetes mellitus (T1DM); MCC950; NLRP3 inflammasome; histopathology

1. Introduction

Diabetic cardiac autonomic neuropathy (DCAN) represents a significant complication of type 1 diabetes mellitus (T1DM) with far-reaching implications for cardiovascular health [1]. In T1DM, the autonomic nervous system, responsible for regulating involuntary bodily functions including heart rate and blood pressure, becomes dysregulated. DCAN manifests as a progressive dysfunction of autonomic nerve fibers innervating the heart and blood vessels, leading to abnormalities in heart rate variability, impaired baroreflex sensitivity, and altered vascular responses [2]. These disruptions

 doi:10.20944/preprints202409.1907.v

contribute to an increased risk of arrhythmias, myocardial ischemia, and sudden cardiac death, underscoring the clinical importance of understanding and managing DCAN in T1DM patients [3].

Extensive research has been conducted to unravel the intricate histopathology of DCAN in T1DM. Studies have implicated multiple mechanisms, including inflammation, endothelial dysfunction, and neurohormonal imbalance, in the development and progression of DCAN [4]. Chronic hyperglycaemia promotes the formation of advanced glycation end-products (AGEs) and activates inflammatory pathways, leading to neuronal damage and dysfunction within the autonomic nervous system. Furthermore, dysregulation of neurohormonal signalling, such as increased sympathetic activity and blunted parasympathetic function, exacerbates cardiac dysautonomia and perpetuates the vicious cycle of DCAN progression [5].

Despite advances in understanding DCAN histopathology, therapeutic options for preventing or reversing its progression remain limited. Current approaches primarily focus on glycaemic control, and lifestyle modifications to mitigate cardiovascular risk factors associated with T1DM [6]. However, these strategies often fail to address the underlying neurodegenerative processes driving DCAN, highlighting the need for novel therapeutic interventions.

One promising avenue of research involves the investigation of MCC950, a potent inhibitor of the NLRP3 inflammasome, in the treatment of DCAN. The NLRP3 inflammasome is a key mediator of inflammation and oxidative stress implicated in the pathogenesis of diabetes and its complications [7,8]. Preclinical studies have shown that MCC950 administration attenuates inflammatory responses, preserves autonomic function, and improves cardiovascular outcomes in diabetic animal models [9]. By targeting the inflammatory cascade underlying DCAN histopathology, MCC950 holds promise as a novel therapeutic agent for preventing or delaying the onset of DCAN and its associated complications in T1DM patients.

Moreover, investigations into the structural alterations within key anatomical structures such as the stellate ganglia, thoracic aorta, and left ventricle have provided valuable insights into the pathological changes associated with DCAN [10]. Diabetes type I induction in Wistar rats, commonly achieved through Streptozotocin (STZ) injections, mimics the hyperglycaemic state observed in T1DM patients and facilitates the study of DCAN progression [11]. Blood pressure and heart rate monitoring techniques allow for the assessment of autonomic dysfunction and cardiovascular abnormalities associated with DCAN [2]. Noradrenaline measurement serves as a marker of sympathetic activity and provides insight into the dysregulation of neurohormonal signalling in DCAN [6]. Dissection and histological examination of the stellate ganglia, thoracic aorta, and left ventricle reveal structural alterations indicative of neuronal damage, vascular remodelling, and myocardial fibrosis characteristic of DCAN [12]. Haematoxylin and Eosin staining elucidate morphological alterations [13], while Masson Trichrome staining highlights collagen deposition and fibrotic changes within the myocardium and blood vessel walls, providing further insights into the structural remodelling underlying DCAN progression [14]. These histological techniques offer valuable tools for characterizing the histopathological changes associated with DCAN and evaluating the efficacy of novel therapeutic interventions, such as MCC950 [10].

The objectives of this study are twofold: first, to elucidate the histopathological mechanisms underlying DCAN in T1DM, focusing on the role of the autonomic nervous system and its interaction with diabetic metabolic derangements; second, to evaluate the therapeutic potential of MCC950, an anti-inflammasome agent, in attenuating DCAN progression in a preclinical model. By addressing these objectives, we aim to contribute to a more comprehensive understanding of DCAN in T1DM and provide insights into novel therapeutic avenues for its management. Through rigorous experimentation and analysis, we seek to bridge the current gaps in knowledge and pave the way for improved clinical outcomes for T1DM patients at risk of DCAN-related complications.

2. Materials and Methods

2.1. Animals

Male Wistar rats weighing between 180-200g were procured from the Comparative Medicine and Technology Unit (COMeT). Ethical approval for animal handling was obtained from the

 doi:10.20944/preprints202409.1907.v

Institutional Animal Care and Use Committee (IACUC). The rats were housed in the Animal Behaviour Laboratory within the Human Anatomy Department, in sanitized cages under controlled environmental conditions, maintaining a 12-hour light/dark cycle, regulated temperature, and humidity levels. A period of two weeks was allotted for the rats to acclimatize to their new environment before the commencement of the experiments. Throughout the adaptation phase, the rats were accommodated in pairs in wooden cages and provided ad libitum access to standard rat pellets [15].

2.2. Diabetes Type I Induction

Following the adaptation period, the rats were randomly assigned to two groups: a Control group (n=10) and an experimental (Type 1 DM model) group (n=10). The DM group received intraperitoneal injections of a high dose of STZ at 50mg/kg [11]. Subsequently, while maintaining their regular diet and housing conditions, all diabetic rats remained untreated until the onset of DCAN was established.

Before the morning blood glucose assessment using an Accu-check Guide Meter glucometer, rats underwent fasting starting from 20:00 the preceding evening. Blood glucose levels were monitored at specific intervals: Week 0, Week 3, Week 16, Week 17, and Week 18. Blood samples were obtained from the tail of each rat following sterilization with an alcohol swab. A small section (approximately 3 mm) of the tail tip was excised, and the blood glucose test paper was inserted into the glucometer for analysis [16]. Each blood glucose measurement was performed in triplicate for each rat to ensure accuracy.

The onset of diabetes in the experimental animals was considered triggered when fasting blood glucose levels exceeded 250 mg/dL (13.9 mmol/L). This threshold was based on established criteria for diabetes induction in rodent models [17].

2.3. Noradrenaline (NA) Measurement

Following appropriate anaesthesia induction with the ketamine/xylazine recipe delivering 80 mg/kg ketamine and 8 mg/kg xylazine, these formulations were prepared in sterile vials using specified dilutions of stock drugs and 0.9% saline diluent. They were then administered intraperitoneally at a dosage of 0.1 mL/100 g [18]. Afterward, 0.5 ml of normal saline was administered intraperitoneally to prevent cannibalism. Whole blood samples for NA measurement were collected using disposable test tubes in accordance with the manufacturer's instructions (Elabscience Biotechnology, China) at Week 10 and Week 14. The rats exhibited a reversal of sedative effects within 2 hours simultaneously. The competitive ELISA principle was employed by the ELISA kit utilized. The provided ELISA plate had been pre-coated with Noradrenaline/Norepinephrine (NA/NE). During the reaction, NA in the samples or standard competed with a fixed amount on the solid-phase supporter for sites on the Biotinylated Detection Ab Specific to NA. Subsequently, excess conjugate and unbound samples were thoroughly washed from the plate, and Avidin conjugated to Horseradish Peroxidase (HRP) was introduced into the microplate well and allowed to incubate. Following this, the TMB substrate solution was added to each well. The enzyme-substrate reaction was halted by the addition of a stop solution, and the resulting colour change was spectrophotometrically measured at a wavelength of 450 nm. The concentration of NA in the samples was determined by comparing the optical density (OD) of the samples to the standard curve (Al-Assi et al., 2018). Each sample was measured in duplicate to ensure reliability.

2.4. MCC950 Treatment

After the establishment of DCAN was confirmed by the evidence of increased NA levels in the experimental group [13], they were randomly subdivided into three subgroups: positive control, treatment, and untreated groups. The initial control group remained as the negative control group. The positive control group received insulin at 5.0 U/kg/day (Zhu et al., 2018), the treatment group

 doi:10.20944/preprints202409.1907.v

was administered IP MCC950 at 3mg/kg/day [19,20], and the untreated group received normal saline 5mg/kg. All groups were administered intraperitoneally for 14 days (**Figure 1**).

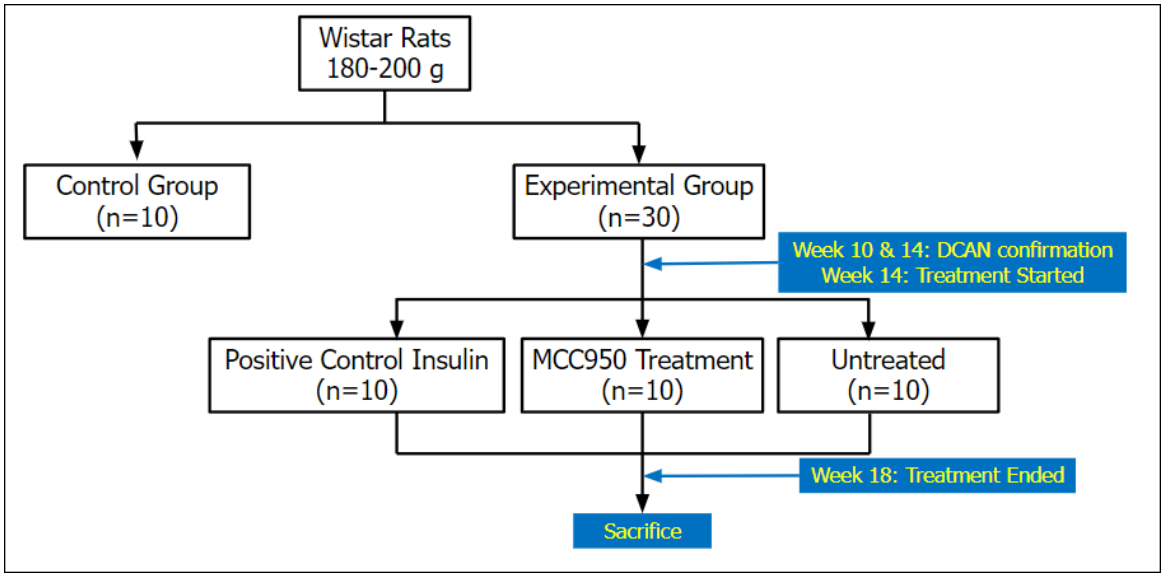

Figure 1. The schematic diagram illustrated four groups of rats: a non-diabetic control group, an experimental diabetic positive control group treated with insulin, treated with MCC950, and an untreated diabetic group, with n=10 in each group.

2.5. Stellate Ganglia, Thoracic Aorta and Left Ventricle Dissection

The stellate ganglia, thoracic aorta, and left ventricle dissection procedures were meticulously conducted with the aid of Motic's stereoscopic microscope to elucidate the structural and histological changes associated with DCAN in Wistar rats [21]. Each tissue type was sampled from 10 rats per group for histological analysis. Following sacrifice, induced by administering a dosage similar to that of the sedative group but without normal saline, the rats were positioned supine, and a midline incision was made along the ventral abdomen to expose the thoracic cavity. Careful attention was given to minimize tissue trauma and maintain physiological integrity throughout the dissection process.

The stellate ganglia were located bilaterally adjacent to the base of the heart, in close proximity to the sympathetic trunk [22]. Using fine dissection scissors and forceps, the stellate ganglia were carefully dissected free from surrounding connective tissue and excised (**Figure 2**). Special care was taken to preserve the anatomical integrity of the ganglia to facilitate subsequent histological analysis.

 doi:10.20944/preprints202409.1907.v

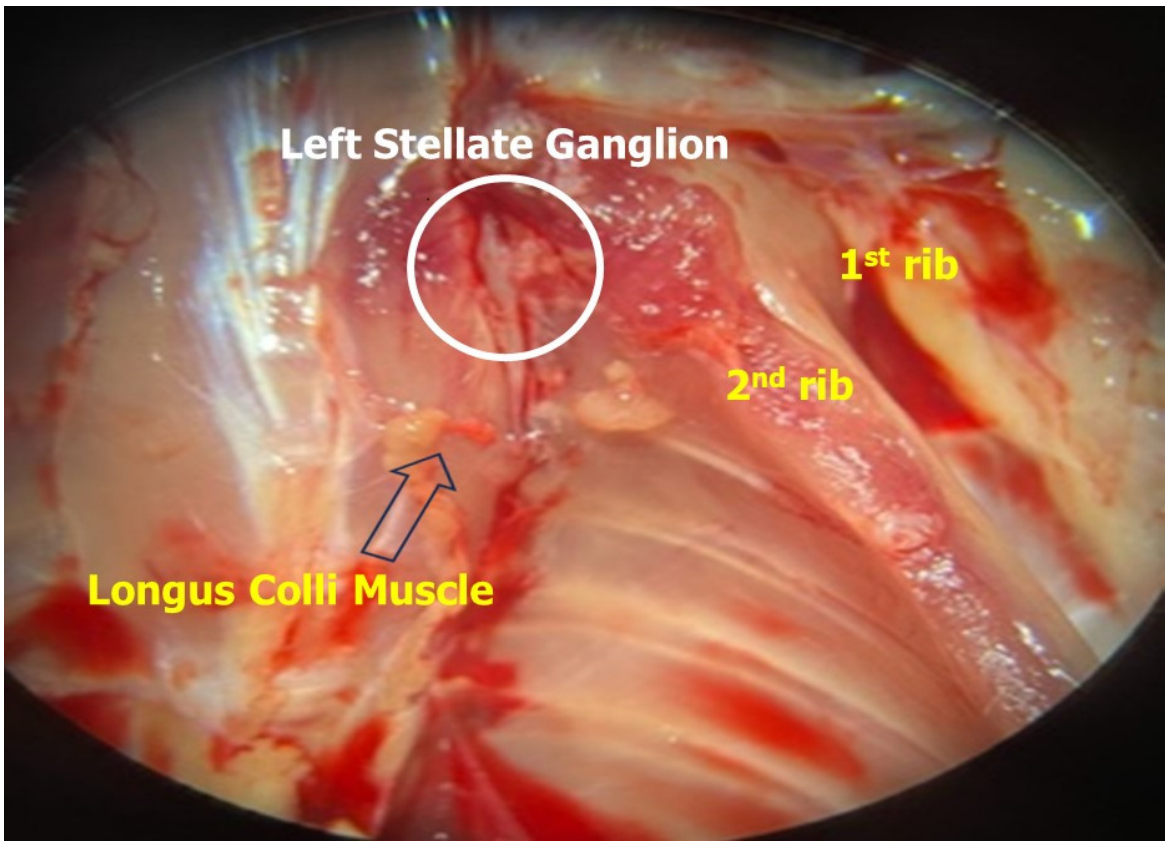

Figure 2. After sacrifice, the gross features of the dissected left stellate ganglion of the Wistar rats were examined. Careful dissection under microscopy aided in identifying nearby landmarks such as the longus colli muscle, 1st and 2nd rib.

Next, the thoracic aorta was exposed by gently retracting the surrounding tissues, including the lungs and thymus [23]. Once visualized, the aorta was carefully dissected free from the adjacent structures and excised proximally from the aortic arch to distally beyond the diaphragm. Great care was taken to avoid damaging the delicate vascular endothelium during the dissection process to ensure accurate histological assessment of vascular morphology.

Finally, the left ventricle of the heart was accessed by carefully opening the pericardium and retracting the surrounding tissues [23]. The left ventricle was then excised en bloc, ensuring inclusion of the entire ventricular wall. Special attention was paid to avoid disrupting the myocardial architecture and to maintain the structural integrity of the ventricular tissue for subsequent histological examination.

Following dissection, tissue specimens were promptly fixed in appropriate fixatives, such as formalin or paraformaldehyde, to preserve tissue morphology and facilitate histological processing [24]. All rats in each group were dissected for further histological slide analysis.

2.6. Haematoxylin and Eosin Staining

The stellate ganglia and thoracic aorta were collected and preserved in a 10% formalin saline solution for 24 hours before being prepared for staining. The fixed tissues were then transferred to the hardening process using paraffin blocks and cut into sections with a thickness of 5 μm. For histological analysis, the sections were mounted on standard glass slides and stained with Haematoxylin and Eosin [25]. This process was conducted using a Nikon microscope at a magnification of 400X. For the quantitative measurement of the stellate ganglia, the average measurement of the 4-shrinkage gap area of each nerve cell was scored. A minimum of 6 sections per tissue per animal were analyzed to ensure representative sampling.

 doi:10.20944/preprints202409.1907.v

2.7. Masson Trichrome Staining

Following similar preservation and sectioning procedures, paraffin blocks containing the left ventricle were prepared for the analysis of collagen content in the endocardium, perivascular area, and myocardium of the fibrosed left ventricle. Masson's trichrome stain was used on tissue slices of the rat heart for this purpose. Furthermore, quantitative analysis of cardiomyocyte size was conducted using the average width and length of its cross-sectional area per focus area [26]. A minimum of 6 sections per tissue per animal were analyzed to ensure representative sampling.

2.8. Statistical Analysis

Statistical analysis was conducted using PRISM version 19, employing one-way analysis of variance (ANOVA) to compare all four groups of rats. Each experimental measurement was repeated at least three times to ensure statistical robustness. A comparison was considered statistically significant if the p-value was less than 0.05.

3. Results

3.1. The Effects of STZ on Fasting Blood Glucose

Hyperglycaemia was confirmed by Week 2 following the STZ injection. As expected, the negative control group (n=10) displayed normal glucose levels compared to the experimental group (n=30) (**Figure 3**). Glucose levels showed a significant increase from Week 3 through Week 18. Additionally, diabetic rats exhibited increased urine production, resulting in frequent urination and polyuria until Week 18.

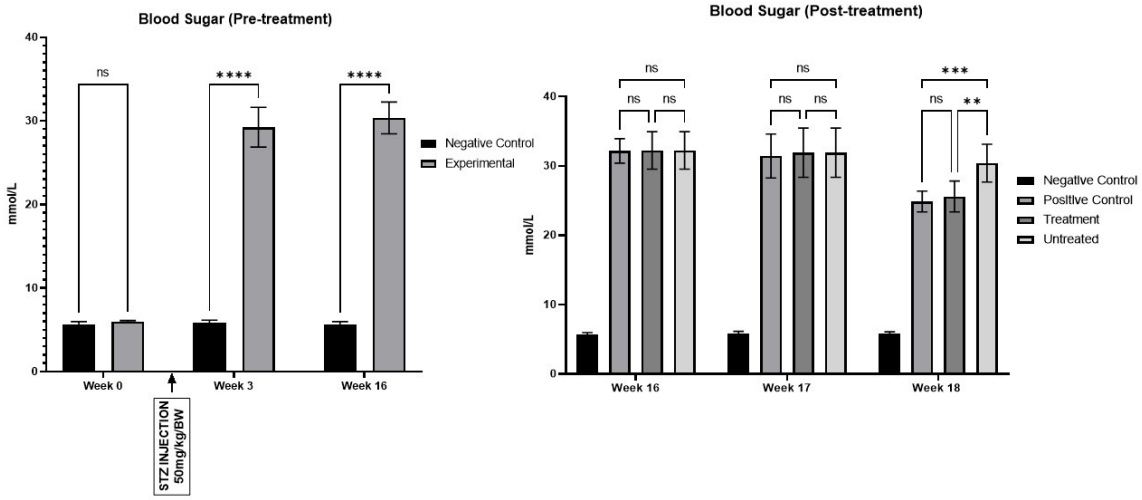

Figure 3. STZ was administered in Week 1, leading to a significant increase in blood glucose levels starting from Week 3 and continuing through Week 16 (****p<0.0001). Post-treatment at Week 18, both the positive control and treatment groups exhibited a significant reduction in blood glucose levels compared to the untreated group, with reductions marked at **p<0.01 and ***p<0.001, respectively.

3.2. The Effects of DM on Serum NA

The ELISA results showed a significant increase in serum NA levels, particularly pronounced in the experimental group compared to the negative control group by week 14 (**Figure 4**). While there was a heightened concentration of NA in Week 10, it did not reach statistical significance. The results at week 14 indicate that the animals were already displaying signs of DCAN.

 doi:10.20944/preprints202409.1907.v

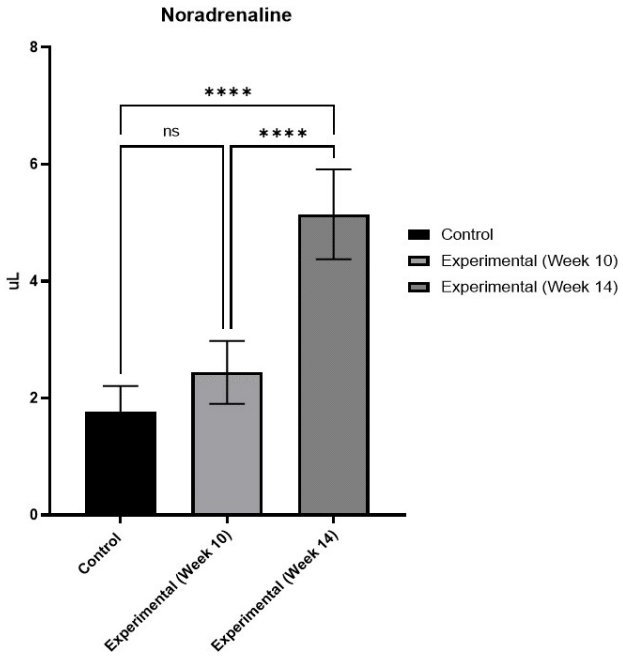

Figure 4. Serum NA levels exhibited a notable rise by Week 14, suggesting the onset of DCAN. No further measurements were undertaken at Week 18 due to limited chemical availability (ns= not significant, ****p<0.0001).

3.3. The Effects of MCC950 on Stellate Ganglia

Histologically, the stellate ganglia showed normal architecture in the negative control group, while the untreated group exhibited atrophy characterized by a decrease in ganglionic size and cell density, reflecting the gradual loss of neurons and structural alterations within the ganglia (**Figure 5**). No obvious shrinkage of the ganglia was observed in the positive control and treatment groups.

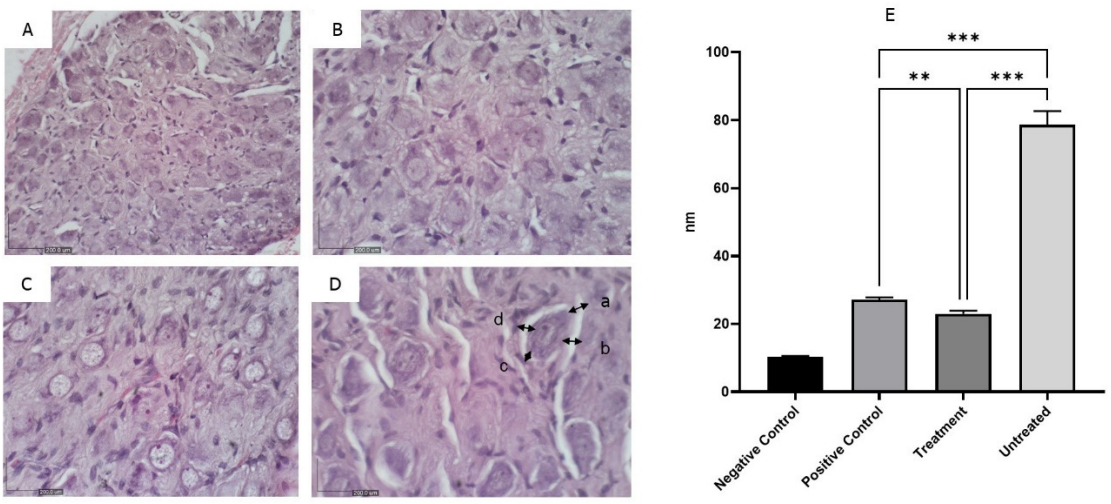

Figure 5. The architecture of the stellate ganglion was measured using four quadrants of each section (a-d), and the average measurement was recorded. The negative control group exhibited normal nerve cells with uniform architecture (A), while the positive control group (B) and treatment group (C) showed minimal shrinkage of nerve cells. In contrast, the untreated group exhibited obvious nerve atrophy characterized by a reduction in ganglionic size (D). The representation (A-D) was depicted in a bar graph, with the untreated group (D) showing significantly greater shrinkage compared to the positive control and treatment groups (***p<0.005) (X400).

 doi:10.20944/preprints202409.1907.v

3.4. The Effects of MCC950 on Thoracic Aorta

The histological examination of the thoracic aorta revealed robust elastic tissue, intact endothelium, and healthy smooth muscle cells in the negative control group (**Figure 6A**). In contrast, the positive control group demonstrated moderate preservation of smooth muscle cells with noticeable cytoplasm clearing (**Figure 6B)**. The MCC950 treatment group exhibited minimal disruption of the endothelial layer and a restoration of smooth muscle integrity (**Figure 6C)**. However, the untreated group displayed significant endothelial damage, characterized by endothelium breakdown, cytoplasmic clearance in smooth muscle cells, and sub-medial separation (**Figure 6D)**.

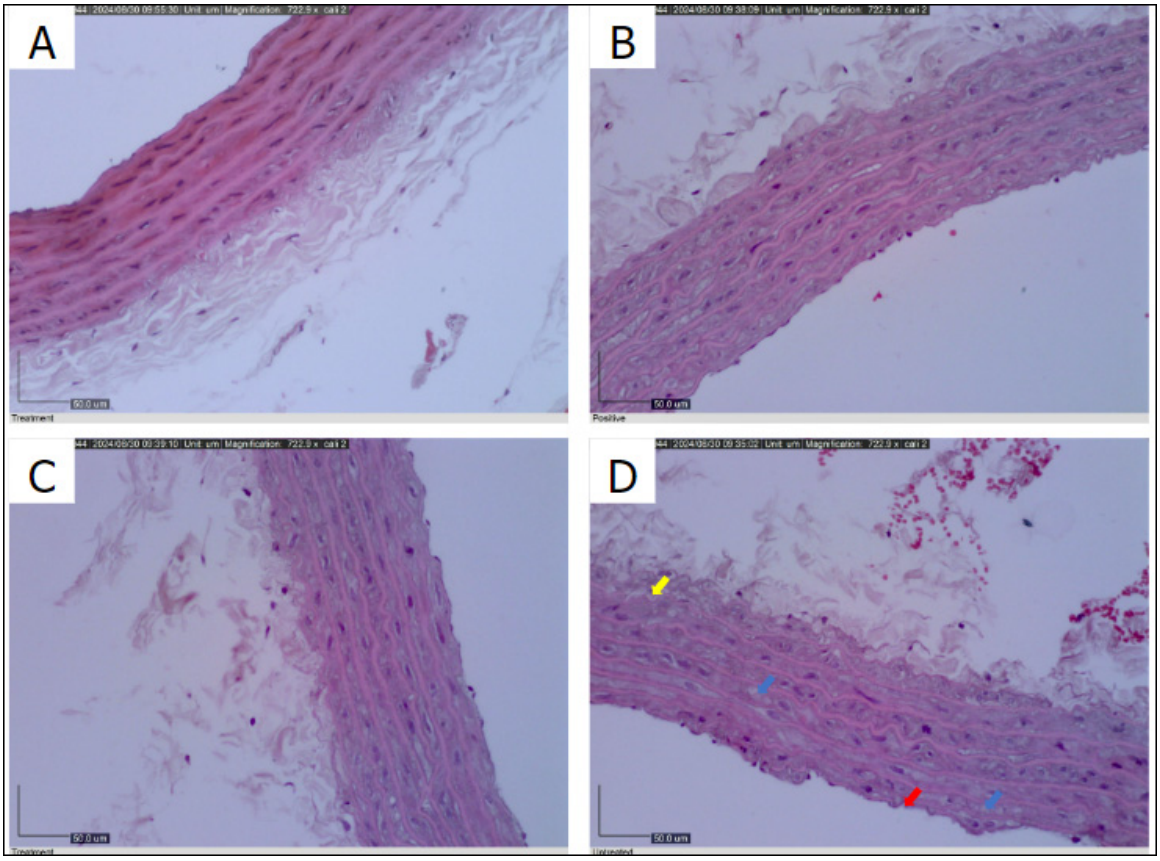

Figure 6. Untreated group (D) exhibits intimal endothelium breakdown (red arrow), cytoplasmic clearance of smooth muscle cells (blue arrow), and sub-medial separation suggesting endothelial damage (yellow arrow), less seen in MCC950 treated (C) (X400).

3.5. The Effects of MCC950 on Left Ventricle

The Masson trichrome histological examination of the left ventricle revealed the presence of fibrosis, evidenced by collagen deposition (blue staining), in the endocardium, perivascular area, and myocardium (**Figure 7**). This staining was markedly prominent in the untreated group. Furthermore, the overall myocardial structure, including the arrangement of cardiac muscle fibers, was found to be altered in the diabetic group of rats (**Figure 8**).

 doi:10.20944/preprints202409.1907.v

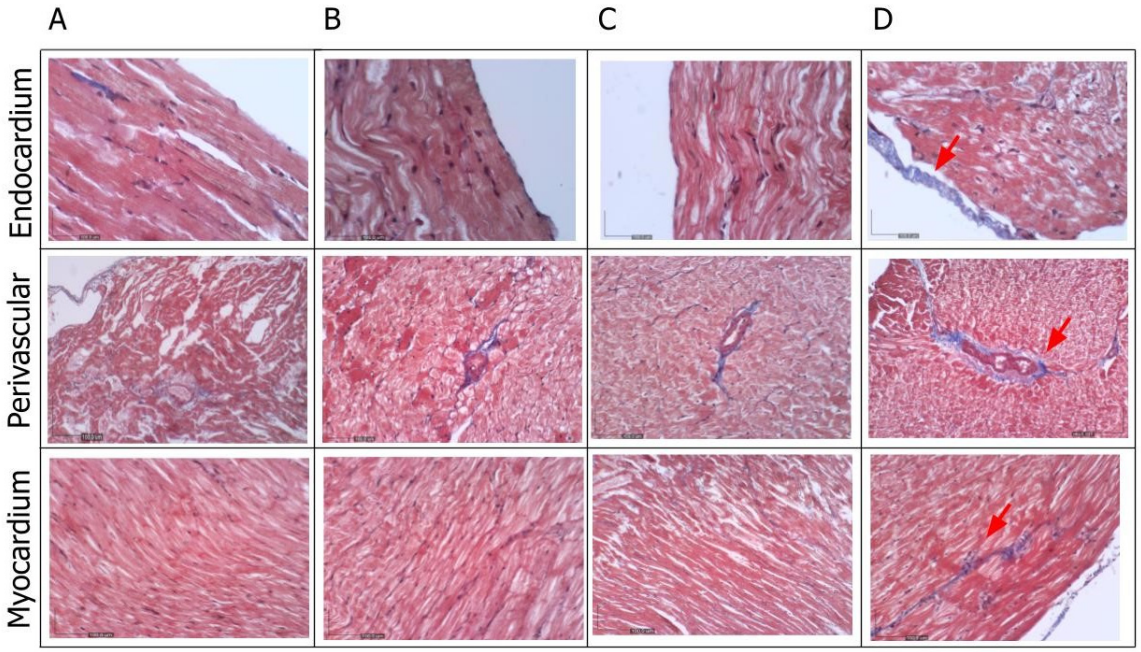

Figure 7. The qualitative analysis of the Masson trichrome staining revealed the least collagen deposition in the negative control group (A), observed in the endocardium, perivascular area, and myocardium. Although there was similar blue staining intensity in both the positive control (B) and treatment group (C), the intensity of staining (red arrow) was markedly more evident in the untreated group (D) (X400).

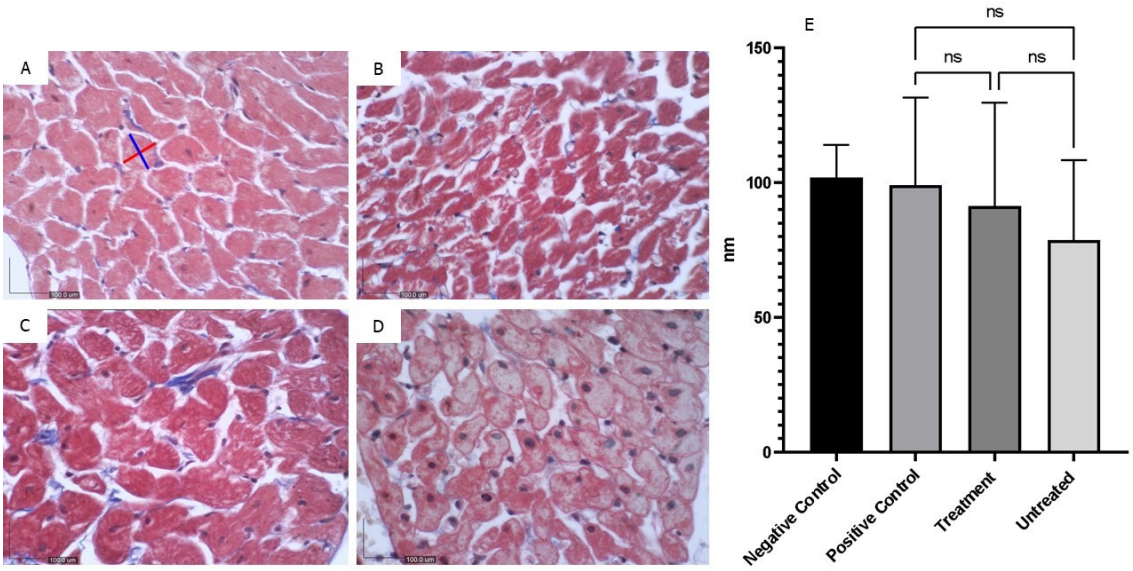

Figure 8. The cross-sectional area of each cardiomyocyte within a focused microscopy area was measured by averaging the length (measured along the blue line) and width (measured along the red line). The negative control group (A) exhibited normal cardiac tissue. Increasing evidence of cardiomyocyte atrophy was observed in the positive control (B), treatment (C), and untreated group (D), respectively. However, these changes were not statistically significant (E) (X400).

 doi:10.20944/preprints202409.1907.v

4. Discussion

The results obtained from this study underscore the profound impact of streptozotocin administration on fasting blood glucose levels in the experimental rat model of type 1 diabetes mellitus. Hyperglycaemia, a hallmark of T1DM, was successfully induced as early as Week 2 post-STZ injection, persisting throughout the observation period until Week 18. This robust and sustained elevation in blood glucose levels is consistent with clinical observations in diabetic patients and validates the effectiveness of STZ as a pharmacological agent for T1DM induction [11]. Moreover, the observed increase in urine production and polyuria in diabetic rats further supports the establishment of T1DM and underscores the physiological consequences of uncontrolled hyperglycaemia [27].

The concomitant rise in serum NA levels in diabetic rats compared to controls by Week 14 provides additional evidence of DCAN onset. The significant elevation in serum NA levels, a hallmark of sympathetic nervous system dysfunction, is indicative of DCAN progression and underscores the utility of NA as a biomarker for autonomic dysfunction in T1DM [28]. Our results align with these findings, reinforcing the association between hyperglycaemia and autonomic imbalance. Although the increase in serum NA levels at Week 10 did not reach statistical significance, the subsequent rise by Week 14 suggests a progressive deterioration of autonomic function in diabetic rats, highlighting the importance of timely intervention to mitigate DCAN-associated complications [29]. Additionally, similar previous study has reported increased NA levels in diabetic subjects, linking elevated sympathetic activity to DCAN and highlighting the progressive nature of autonomic dysfunction in diabetes [30].

Histological examination of the stellate ganglia revealed significant structural alterations in untreated diabetic rats, characterized by neuronal atrophy and decreased ganglionic size and cell density [10]. These observations are in line with those reported previously who documented similar neuronal damage and atrophy in the autonomic ganglia of diabetic rodents, emphasizing the neurodegenerative impact of chronic hyperglycaemia [31]. In contrast, treatment with MCC950 preserved ganglionic architecture, thereby mitigating neuronal damage and structural alterations within the ganglia. These findings underscore the therapeutic potential of MCC950 in preserving autonomic nerve function and preventing DCAN progression [32].

Similarly, MCC950 treatment attenuated endothelial damage and restored smooth muscle integrity in the thoracic aorta, as evidenced by histological examination. Previous studies has shown that diabetes induces endothelial dysfunction and vascular damage, characterized by impaired endothelial-dependent relaxation and increased oxidative stress [33]. Our results demonstrate that MCC950 can counteract these effects, restoring vascular integrity and function, which is consistent with its known anti-inflammatory and antioxidant properties [34].

Furthermore, Masson trichrome staining of the left ventricle revealed marked fibrosis in untreated diabetic rats, indicative of adverse cardiac remodelling and myocardial damage. Previous study has highlighted the role of hyperglycaemia-induced oxidative stress and inflammation in promoting myocardial fibrosis in diabetes, leading to compromised cardiac function [35]. Our findings suggest that MCC950 treatment attenuates collagen deposition and preserves myocardial structure, offering a potential therapeutic avenue for mitigating cardiac fibrosis in DCAN [36].

Overall, the findings of this study provide valuable insights into the histopathological mechanisms underlying DCAN and highlight the therapeutic potential of MCC950 in attenuating DCAN progression. Our results are consistent with previous research on the detrimental effects of hyperglycaemia on autonomic and cardiovascular health and support the potential of MCC950 as a novel therapeutic agent for DCAN. Further research is warranted to elucidate the molecular mechanisms underlying MCC950's therapeutic effects and validate its efficacy in human trials, ultimately leading to improved clinical outcomes for T1DM patients at risk of DCAN-related complications.

While the study provides valuable insights into the histopathological mechanisms of DCAN and the potential therapeutic effects of MCC950, it primarily relies on preclinical animal models.

 doi:10.20944/preprints202409.1907.v

Translating these findings into clinical applications for human patients may pose challenges due to interspecies variations and the complexity of human physiology compared to animal models.

The study's duration, particularly the treatment period with MCC950, is relatively short. The long-term effects and safety profiles of MCC950 in the context of DCAN management remain unclear. Further investigation with extended observation periods could provide more comprehensive insights into the therapeutic efficacy and potential adverse effects.

Furthermore, the sample size in the experimental groups, particularly for the treatment with MCC950, is relatively small. A larger sample size would enhance the statistical power and generalizability of the findings. Additionally, subgroup analyses based on factors such as age, gender, and disease severity could provide deeper insights into treatment responses.

The study primarily focuses on investigating the therapeutic potential of MCC950 in attenuating DCAN progression. While MCC950 targets inflammation, DCAN is a multifactorial condition influenced by various histopathological mechanisms. Exploring combination therapies or alternative treatment modalities targeting different pathways could offer a more comprehensive approach to DCAN management.

The study relies solely on histological evaluations to assess structural and histopathological changes associated with DCAN and the effects of MCC950 treatment. While histological analyses provide valuable insights, integrating functional assessments such as electrocardiography (ECG), echocardiography, and autonomic function tests could offer a more comprehensive understanding of DCAN progression and treatment responses.

Addressing these limitations in future research endeavours could enhance the validity and clinical applicability of the study findings, ultimately contributing to improved management strategies for DCAN in T1DM patients.

5. Conclusion

In conclusion, the observed elevation in serum noradrenaline levels by Week 14 provides further evidence of diabetic cardiac autonomic neuropathy onset, highlighting the progressive deterioration of autonomic function in diabetic rats. Histological examination revealed significant structural alterations in the stellate ganglia, thoracic aorta, and left ventricle of untreated diabetic rats, indicative of neuronal damage, vascular dysfunction, and myocardial fibrosis characteristic of DCAN. However, treatment with MCC950 demonstrated promising therapeutic potential in preserving autonomic nerve function, mitigating vascular damage, and attenuating cardiac fibrosis in diabetic rats. These findings underscore the need for further research to elucidate the molecular mechanisms underlying MCC950's therapeutic effects and validate its efficacy in human trials, ultimately offering new avenues for the management of DCAN and improving clinical outcomes for T1DM patients.

Authors' Contribution: SDS performed the literature review, data curation, data collection, and visualization of results. JC, ZAB, WKH and MAK conducted data collection, statistical analysis, and drafted the initial methods section. RA was responsible for conceptualization, funding acquisition, study design, writing the original draft, and final manuscript editing.

Data Availability Statement: The datasets generated and/or analyzed during the current study are available from the corresponding author on reasonable request.

Acknowledgments: We extend our gratitude to the dedicated staff members from both departments whose invaluable assistance was instrumental in accomplishing the laboratory work. Special recognition is given to the supporting grant GP/IPM/2022/9739600 and the ethical approval UPM/IACUC/AUP-R015/2023.

Conflicts of Interest: None.

References

1. El Tantawy, A., et al., Cardiac autonomic neuropathy linked to left ventricular dysfunction in type 1 diabetic patients. Cardiovascular Endocrinology & Metabolism, 2022. **11**(4): p. e0272.
2. Sudo, S.Z., et al., Diabetes-induced cardiac autonomic neuropathy: impact on heart function and prognosis. Biomedicines, 2022. **10**(12): p. 3258.

 doi:10.20944/preprints202409.1907.v

3. Svane, J., U. Pedersen-Bjergaard, and J. Tfelt-Hansen, *Diabetes and the risk of sudden cardiac death.* Current cardiology reports, 2020. **22**: p. 1-10.
4. Bakkar, N.-M.Z., et al., Cardiac autonomic neuropathy: a progressive consequence of chronic low-grade inflammation in type 2 diabetes and related metabolic disorders. International journal of molecular sciences, 2020. **21**(23): p. 9005.
5. Williams, S., et al., Cardiac autonomic neuropathy in type 1 and 2 diabetes: epidemiology, pathophysiology, and management. Clinical therapeutics, 2022. **44**(10): p. 1394-1416.
6. Serhiyenko, V. and A. Serhiyenko, Diabetic cardiac autonomic neuropathy, in The Diabetes Textbook: Clinical Principles, Patient Management and Public Health Issues. 2023, Springer. p. 939-966.
7. Razif, A., et al., The Evolving Role of Nucleotide-binding Oligomerisation Domain-like Receptor Pyrin Domain 3 Inflammasome Activation in Vascular Endothelial Cells: A Review. The Malaysian Journal of Medical Sciences: MJMS, 2022. **29**(2): p. 8.
8. Subramaniam, S.D., et al., Diabetic Cardiac Autonomic Neuropathy: A Review of NLRP3 Inflammasome Complicity. Mal J Med Health Sci, 2024. **20**(1): p. 365-368.
9. Wang, M., et al., MCC950, a selective NLRP3 inhibitor, attenuates adverse cardiac remodeling following heart failure through improving the cardiometabolic dysfunction in obese mice. Frontiers in Cardiovascular Medicine, 2022. **9**: p. 727474.
10. Filipović, N., et al., Cardiac innervations in diabetes mellitus—Anatomical evidence of neuropathy. The Anatomical Record, 2023. **306**(9): p. 2345-2365.
11. Ghasemi, A. and S. Jeddi, Streptozotocin as a tool for induction of rat models of diabetes: A practical guide. EXCLI journal, 2023. **22**: p. 274.
12. Dimitropoulos, G., A.A. Tahrani, and M.J. Stevens, *Cardiac autonomic neuropathy in patients with diabetes mellitus.* World journal of diabetes, 2014. **5**(1): p. 17.
13. Akinlade, O.M., B.V. Owoyele, and O.A. Soladoye, Heart rate variability indices, biomarkers, and cardiac nerve density: Independent surrogate markers for diagnosis of diabetic cardiac autonomic neuropathy in type 2 diabetes mellitus animal model. International Journal of Health Sciences, 2020. **14**(6): p. 24.
14. Al-Assi, O., et al., Cardiac autonomic neuropathy as a result of mild hypercaloric challenge in absence of signs of diabetes: modulation by antidiabetic drugs. Oxidative Medicine and Cellular Longevity, 2018. **2018**.
15. Akinlade, O.M., B.V. Owoyele, and A.O. Soladoye, Streptozotocin-induced type 1 and 2 diabetes in rodents: A model for studying diabetic cardiac autonomic neuropathy. African Health Sciences, 2021. **21**(2): p. 719-727.
16. Shi, L., et al., Beneficial Effects of lncRNA-UC. 360+ shRNA on Diabetic Cardiac Sympathetic Damage via NLRP3 Inflammasome-Induced Pyroptosis in Stellate Ganglion. ACS omega, 2022. **7**(31): p. 27714-27721.
17. Li, Z., et al., Elevated glucose metabolism driving pro-inflammatory response in B cells contributes to the progression of type 1 diabetes. Clinical Immunology, 2023. **255**: p. 109729.
18. Oh, S.S. and H.L. Narver, *Mouse and Rat Anesthesia and Analgesia.* Current Protocols, 2024. **4**(2): p. e995.
19. Ni, B., et al., MCC950, the NLRP3 inhibitor, protects against cartilage degradation in a mouse model of osteoarthritis. Oxidative Medicine and Cellular Longevity, 2021. **2021**(1): p. 4139048.
20. Ward, R., et al., NLRP3 inflammasome inhibition with MCC950 improves diabetes-mediated cognitive impairment and vasoneuronal remodeling after ischemia. Pharmacological research, 2019. **142**: p. 237-250.
21. Yu, X.-D., et al., Additions to Occultibambusaceae (Pleosporales, Dothideomycetes): Unrevealing Palmicolous Fungi in China. Diversity, 2021. **13**(11): p. 516.
22. Scherschel, K., et al., *Location, dissection, and analysis of the murine stellate ganglion.* JoVE (Journal of Visualized Experiments), 2020(166): p. e62026.
23. Abas, R., F. Othman, and Z.C. Thent, Protective effect of Momordica charantia fruit extract on hyperglycaemia-induced cardiac fibrosis. Oxidative Medicine and Cellular Longevity, 2014. **2014**.
24. Ajileye, A. and E. Esan, *Fixation and fixatives in histopathology: a review.* Bayero Journal of Pure and Applied Sciences, 2022. **15**(1): p. 231-243.
25. Ahmed, Y.M., et al., Partial Synthetic PPARY Derivative Ameliorates Aorta Injury in Experimental Diabetic Rats Mediated by Activation of miR-126-5p Pi3k/AKT/PDK 1/mTOR Expression. Pharmaceuticals, 2022. **15**(10): p. 1175.
26. Li, H., et al., *A new model of heart failure post-myocardial infarction in the rat.* JoVE (Journal of Visualized Experiments), 2021(172): p. e62540.
27. Vega-Martín, E., et al., Upregulation in Inflammation and Collagen Expression in Perirenal but Not in Mesenteric Adipose Tissue from Diabetic Munich Wistar Frömter Rats. International Journal of Molecular Sciences, 2023. **24**(23): p. 17008.
28. Zhang, L.-Z., et al., Perioperative changes of serum orphanin in diabetic patients and its relationship with sympathetic nervous system. Neuropeptides, 2024. **104**: p. 102414.
29. Carmichael, J., et al., Advances in screening, early diagnosis and accurate staging of diabetic neuropathy. Frontiers in endocrinology, 2021. **12**: p. 671257.

 doi:10.20944/preprints202409.1907.v

30. Voulgari, C., et al., Exercise improves cardiac autonomic function in obesity and diabetes. Metabolism, 2013. **62**(5): p. 609-621.
31. Sima, A.A. and W. Zhang, *Mechanisms of diabetic neuropathy: axon dysfunction.* Handbook of clinical neurology, 2014. **126**: p. 429-442.
32. Amo-Aparicio, J., et al., Inhibition of the NLRP3 inflammasome by OLT1177 induces functional protection and myelin preservation after spinal cord injury. Experimental Neurology, 2022. **347**: p. 113889.
33. Subburathinam, G., A Study of Endothelial Dysfunction, by Flow Medaiated Vasodialation in Diabetic Patients. 2020, Madras Medical College, Chennai.
34. Romero, A., et al., Pharmacological blockade of NLRP3 inflammasome/IL-1β-positive loop mitigates endothelial cell senescence and dysfunction. Aging and disease, 2022. **13**(1): p. 284.
35. Kaur, N., et al., Mechanisms and therapeutic prospects of diabetic cardiomyopathy through the inflammatory response. Frontiers in Physiology, 2021. **12**: p. 694864.
36. Bakhshi, S. and S. Shamsi, MCC950 in the treatment of NLRP3-mediated inflammatory diseases: Latest evidence and therapeutic outcomes. International Immunopharmacology, 2022. **106**: p. 108595.